



## ISTITUTO NAZIONALE DI RICERCA METROLOGICA Repository Istituzionale

Measurement of the neutron flux parameters  $f$  and  $\alpha$  at the Pavia TRIGA Mark II reactor

This is the author's accepted version of the contribution published as:

*Original*

Measurement of the neutron flux parameters  $f$  and  $\alpha$  at the Pavia TRIGA Mark II reactor / Di Luzio, Marco; Oddone, Massimo; Prata, Michele; Alloni, Daniele; D'Agostino, Giancarlo. - In: JOURNAL OF RADIOANALYTICAL AND NUCLEAR CHEMISTRY. - ISSN 0236-5731. - 312:(2017), pp. 75-80. [10.1007/s10967-017-5191-4]

*Availability:*

This version is available at: 11696/54215 since: 2020-05-19T13:54:33Z

*Publisher:*

Springer

*Published*

DOI:10.1007/s10967-017-5191-4

*Terms of use:*

This article is made available under terms and conditions as specified in the corresponding bibliographic description in the repository

*Publisher copyright*

SPRINGER

Copyright © Springer. The final publication is available at [link.springer.com](http://link.springer.com)

(Article begins on next page)

1

## **Title page**

2 Names of the authors: Marco Di Luzio<sup>(1)-(2)</sup>, Massimo Oddone<sup>(2)</sup>, Michele Prata<sup>(3)</sup>,  
3 Daniele Alloni<sup>(3)</sup>, Giancarlo D'Agostino<sup>(1)</sup>

4 Title: Measurement of the neutron flux parameters  $f$  and  $\alpha$  at the Pavia TRIGA Mark II  
5 reactor

6 Affiliation(s) and address(es) of the author(s):

7 (1) Istituto Nazionale di Ricerca Metrologica (INRIM) – Unit of Radiochemistry and  
8 Spectroscopy, University of Pavia, Viale Taramelli 12, 27100 Pavia, Italy

9 (2) Department of Chemistry – Radiochemistry Area, University of Pavia, Viale  
10 Taramelli 12, 27100 Pavia, Italy

11 (3) Laboratorio Energia Nucleare Applicata (LENA), University of Pavia, Via Aselli 41,  
12 27100 Pavia, Italy

13 E-mail address of the corresponding author: m.diluzio@inrim.it

14

15 **Measurement of the neutron flux parameters  $f$  and  $\alpha$  at**  
16 **the Pavia TRIGA Mark II reactor**

17 M. Di Luzio<sup>1-2</sup>, M. Oddone<sup>2</sup>, M. Prata<sup>3</sup>, D. Alloni<sup>3</sup>, G. D'Agostino<sup>1</sup>

18 <sup>1</sup>*Istituto Nazionale di Ricerca Metrologica (INRIM) – Unit of Radiochemistry and*  
19 *Spectroscopy, University of Pavia, Viale Taramelli 12, 27100 Pavia, Italy*

20 <sup>2</sup>*Department of Chemistry – Radiochemistry Area, University of Pavia, Viale Taramelli*  
21 *12, 27100 Pavia, Italy*

22 <sup>3</sup>*Laboratorio Energia Nucleare Applicata (LENA), University of Pavia, Via Aselli 41,*  
23 *27100 Pavia, Italy*

24 **Abstract**

25 In this paper, evaluation of neutron flux parameters of TRIGA Mark II reactor in Pavia  
26 was carried out. For any of the three irradiation positions investigated, this work  
27 represented the first experimental evaluation of  $\alpha$ . Moreover, in addition to  $\alpha$ , values of  
28 other parameters such as  $f$ ,  $C_{th}$  and  $C_{ie}$  were also calculated and compared with the  
29 existent literature data from other TRIGA Mark II reactors and the Pavia's facility.  
30 Results obtained in the present study represent a mandatory step ahead for future  
31 application of  $k_0$ -Neutron Activation Analysis method ( $k_0$ -NAA) at Pavia's facility.

32 **Keywords**

33 Neutron flux parameters, TRIGA Mark II, Cd-cover,  $k_0$  method

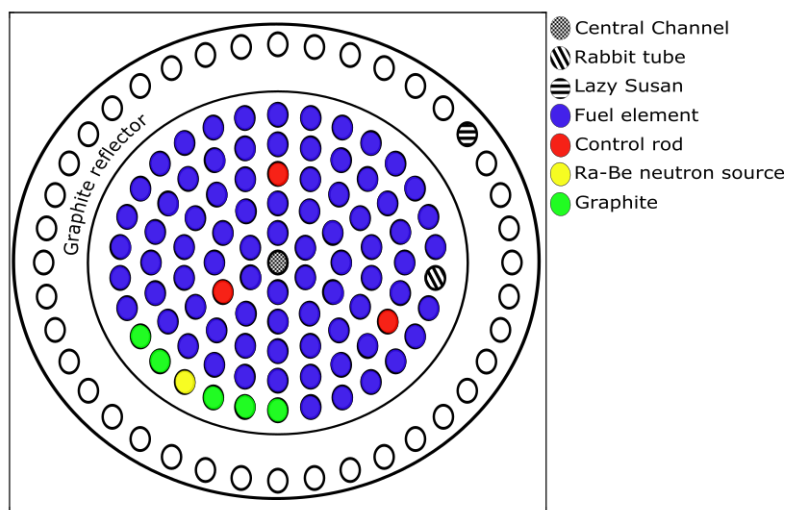
34 **Introduction**

35 In the framework of the application of  $k_0$  standardization method to Neutron Activation  
36 Analysis ( $k_0$ -NAA), reliable knowledge of two parameters of the neutron flux ( $f$  and  $\alpha$ ) is  
37 mandatory [1]. The first one indicates ratio between thermal and epithermal neutron flux  
38 while the second one provides a better representation of epithermal part of neutron  
39 spectrum shape. In this paper, evaluation of these two parameters was accomplished in  
40 three different irradiation channels of reactor TRIGA Mark II of Laboratorio di Energia  
41 Nucleare Applicata (LENA) situated in Pavia, with the aim to introduce the use of  $k_0$ -  
42 NAA in this facility on a permanent basis. In particular: the position 1 (closest to equator)  
43 of Central Channel (i), position number 27 of rotary specimen rack (codenamed Lazy  
44 Susan) (ii) and pneumatic transfer tube (codenamed Rabbit) (iii) (Fig. 1) channel's  
45 factors  $f$  and  $\alpha$  were evaluated with methods based on irradiations with and without Cd  
46 cover.

47 The pool-type facility of Pavia is a 250 kW reactor working with 20% enriched  $^{235}\text{U}$  fuel  
48 elements and moderated with demineralized light water [2].

49

50 **Fig. 1** Cross section representation of TRIGA Mark II reactor channels in



51 Pavia

## 52 Theory

53 Knowledge of  $\alpha$  is of fundamental importance in order to quantify deviation from  $1/E$   
 54 dependence of neutron spectrum in the epithermal range. The energy distribution of the  
 55 neutron flux in the epithermal range,  $\varphi_e(E)$ , in an ideal spectrum varies as  $1/E$  from  
 56 conventional epithermal neutron flux evaluated at 1 eV ( $\Phi_e$ ). In real spectra, however,  
 57 this dependence is not fulfilled due to core configuration and effect of moderator  
 58 elements. In a real situation, the slope of function for epithermal neutrons deviates from  
 59  $1/E$  shape, for this reason a dimensionless correction factor  $\alpha$  has to be taken into account  
 60 according to

$$61 \quad \varphi_e(E) = \Phi_e \frac{1}{E} (1 + \alpha) \quad . \quad (1)$$

63 To achieve experimental evaluation of  $\alpha$  parameter, a series of flux monitors, nuclides  
 64 with defined resonance energies ( $E_r$ ) in the epithermal range, are used as neutron flux  
 65 spots in the investigated region. In this case use of effective resonance energies ( $\bar{E}_r$ ) is  
 66 mandatory because they represent the energy of a fictitious single-resonance which  
 67 provides the same activation rate of all epithermal resonances of the nuclide. In addition,  
 68 they allow to consider the effect of  $\alpha$  on resonance integrals according to

$$69 \quad \bar{E}_r^{\alpha} I'_0(\alpha) = I'_0, \quad (2)$$

70 where  $I'_0$  and  $I'_0(\alpha)$  are the reduced resonance integral in the case of ideal and real  
 71 neutron spectrum, respectively [3].

72 From eq. (1), appearance of the epithermal production rate per target nucleus ( $R_e$ ),  
 73 defined as  $R_e = F_{Cd} G_{Cd} \Phi_e I'_0(\alpha)$ , can be deduced.  $R_e$  indicates the amount of  
 74 radionuclide produced per target nucleus per second in the nuclear reactor that is  
 75 expected when a cut-off is applied to the thermal component of neutron flux, as happens  
 76 in an irradiation performed under Cd cover;  $R_e$  is straightly connected with specific  
 77 activity ( $A_{sp,Cd}$ ), where the subscript Cd denotes the presence of Cd-cover. In particular,

$$78 \quad R_e = \frac{M A_{sp,Cd}}{N_A \theta(\varepsilon_p)}$$

79 detection of delayed  $\gamma$ -rays with gamma spectrometry; where  $M$  is the molar mass,  $N_A$  is

80 the Avogadro constant,  $\theta$  is the isotopic abundance of target nuclide,  $\Gamma$  is the  $\gamma$  yield for  
 81 100 disintegrations,  $\varepsilon_p$  is the detector efficiency at full-energy peak.

82 Accordingly,  $\varphi_e(\bar{E}_r)$  can be defined as follows

$$83 \quad \varphi_e(\bar{E}_r) = \frac{\bar{E}_r^{-\alpha} M A_{sp,Cd}}{N_A \theta F_{Cd} G_e (\varepsilon_p \bar{E}_r I_0(\alpha))}, \quad (3)$$

84 where  $A_{sp,Cd} = \frac{N_p/tl}{SDCW}$ ;  $N_p$  is the net count of full energy peak corrected for coincidence  
 85 losses;  $S = 1 - e^{-t_i}$ , is the saturation factor;  $D = e^{-t_{td}}$ , is the decay factor;  
 86  $C = (1 - e^{-t_c}) / (t_c)$ , is the counting factor;  $tl$ ,  $t_c$ ,  $t_i$ ,  $t_d$  are the live time of spectrum  
 87 collection, real time of spectrum collection, irradiation time and time interval between  
 88 irradiation and counting respectively;  $\lambda$  is the decay constant of the produced  
 89 radionuclide;  $w$  is the mass of monitor element.  $I_0(\alpha)$  is the resonance integral taking into  
 90 account variation of epithermal neutron flux from ideal shape  $1/E$ ;  $F_{Cd}$  is a correction  
 91 factor taking into account the shielding of epithermal flux due to Cd cover;  $G_e$  is  
 92 epithermal self-shielding effect due to the sample.

93 Moreover,  $k_0$  factors can be successfully deducted.  
 94  $k_1(0, Au)(i) = (M_{1Au} \theta_{1i} \sigma_1(0, i) (i)) / (M_{1i} \theta_{1Au} \sigma_1(0, Au) (iAu))$ , from definition of  $k_0$   
 95 comparator, where  $\sigma_0$  is the (n, $\gamma$ ) cross section at 2200 m s<sup>-1</sup> neutron speed and subscript  $i$   
 96 denotes parameters referred to analyte of interest while subscript Au refers to gold, the  
 97 ultimate comparator. With inclusion of  $k_0$  factor  $\varphi_e(\bar{E}_r)$  can be represented as follows:

$$98 \quad \varphi_e(\bar{E}_r) \bar{E}_r = \frac{\bar{E}_r^{-\alpha} A_{sp,Cd} nk}{k_{0,Au}(i) F_{Cd} G_e \varepsilon_p Q_0(\alpha)} \quad (4)$$

99 Where  $nk$  represents a factor composed by  $N_A$  and nuclear parameters,

100  $nk = M_{1Au} / (\theta_{1Au} \sigma_1(0, Au) (iAu) N_{1A})$ , and  $Q_0(\alpha)$  is the ratio of  $I_0(\alpha)$  to  $\sigma_0$ .

101 Application of logarithm to eq. (4) shows the linear dependence between  $\log \varphi_e(\bar{E}_r) \bar{E}_r$   
 102 and  $\log \bar{E}_r$ , with the first representing the dependent variable and the latter the  
 103 independent variable:

$$104 \quad \log \left[ \varphi_e(\bar{E}_r) \bar{E}_r \right] = -\alpha \log \bar{E}_r + \log \frac{A_{sp,Cd} nk}{k_{0,Au}(i) F_{Cd} G_e \varepsilon_p Q_0(\alpha)}. \quad (5)$$

105 The Cd-cover method is suitable to determine  $\alpha$  via eq. (5) by irradiating a set of  
 106 monitors under a Cd cover and following counting of gamma emitted, through gamma  
 107 spectrometry.

108 A monitor set with a wide and well distributed energy range is recommended to be  
 109 chosen; for each monitor element, after irradiation and counting, eq. (5) can be applied  
 110 using an initial guess value for  $\alpha$  ( $\alpha=0$ ). Results can be plotted on a  $\log(\Phi_e(\bar{E}_r)\bar{E}_r)$  to  
 111  $\log(\bar{E}_r)$  graph and the slope of the straight line resulting from an iterative least-square  
 112 regression fit leads to the determination of  $\alpha$  [4].

113 For what concerns the measurement of  $f$ , a comparison between obtained activity from a  
 114 similar monitor set deriving from the covered irradiation and a bare one can be

115 performed. The cadmium ratio  $R_{Cd} = \frac{A_{sp,b}}{A_{sp,Cd}}$ , where  $A_{sp,b}$  is defined as specific activity after  
 116 a bare irradiation, corresponds to

$$117 \quad R_{Cd} = \frac{G_{th}(\Phi_{th} \sigma_{t0} + G_{th} \Phi_{th} I_{t0}(\alpha))}{G_{th} \Phi_{th} I_{t0}(\alpha) F_{Cd}} \quad (6)$$

119 where  $\Phi_{th}$  is the conventional thermal neutron flux and  $G_{th}$  is the self-shielding factor of  
 120 the sample for thermal neutrons.

121 Consequently,  $f$  can be obtained from  $R_{Cd}$  for each monitor [5] according to

$$122 \quad f = \frac{G_e}{G_{th}} Q_0(\alpha) (R_{Cd} F_{Cd} - 1) \quad (7)$$

123 Moreover,  $\Phi_e$  can be obtained from eq. (4). In fact, according to eq. (1),  
 124  $\Phi_e = \Phi_{th} \Phi_e(E) E^{\alpha} (1 + \alpha)$ , that leads to

$$125 \quad \Phi_e = \frac{A_{sp}(sp, Cd) \cdot nk}{[k_{th}(0, Au) \cdot (F_{Cd} G_{th}) \cdot \Phi_{th} \sigma_{t0}(\alpha)]} \quad (8)$$

127 It means that the value of  $\Phi_e$  can be determined by calculating eq. (8) on each monitor  
 128 element. Thus, from the knowledge of  $f$ , also  $\Phi_{th}$  is derived from

$$129 \quad \Phi_{th} = \Phi_e f \quad (9)$$

## 130 **Experimental**

131 A similar monitor mixture composed by Au, Co, Zr and Rb was used. The amount of  
 132 each monitor element was adjusted in order to obtain adequate activity with respect to the  
 133 irradiation position. This monitor set allowed investigation on epithermal part of flux  
 134 ranging from 5.65 to 6260 eV. (Table 1) provides information about relevant parameters  
 135 of selected monitor elements.

136

137 **Table 1** List of elements combined in a monitor set, all data were taken from [6] but  $F_{Cd}$   
 138 [7]. The  $F_{Cd}$  value for Rb was assumed as 1 because its  $\bar{E}_r$  is distant enough from  $E_{Cd}$  to  
 139 not perceive perturbation in epithermal part of flux at resonance energy. The standard  
 140 uncertainties in parentheses apply to the last digits.

Monitor	$\bar{E}_r / \text{eV}$	$Q_0$	$t_{1/2}$	$E / \text{keV}$	$k_{0,Au}(\alpha)$	$F_{Cd}$
$^{197}\text{Au}(n, \gamma)^{198}\text{Au}$	5.7(4)	15.7(3)	2.6950(2) days	411.8	1	0.991
$^{59}\text{Co}(n, \gamma)^{60}\text{Co}$	136(7)	1.99(6)	1925.3(3) days	1332.5	1.320(7)	1
$^{85}\text{Rb}(n, \gamma)^{86}\text{Rb}$	839(50)	14.8(4)	18.63(2) days	1077.0	$7.65(8) \times 10^{-4}$	1
$^{94}\text{Zr}(n, \gamma)^{95}\text{Zr}$	6260(250)	5.31(18)	64.02(6) days	756.7	$1.10(1) \times 10^{-4}$	1

141

142 A standard solution was used for Co (1000  $\mu\text{g mL}^{-1}$ , VWR Chemicals) and Rb (1000  $\mu\text{g}$   
 143  $\text{mL}^{-1}$ , VWR Chemicals), while in the case of Zr, discs (0.992  $\text{g g}^{-1}$  mass fraction, 6 mm  
 144 diameter and 0.1 mm thickness, ZR000260 GoodFellow) were preferred. For Au, a 100  
 145  $\mu\text{g mL}^{-1}$  solution (diluted from a 1000  $\mu\text{g mL}^{-1}$  standard solution, VWR Chemicals) or an  
 146 Al-Au(0.1%, IRMM-530RA) foil 0.1 mm thickness were used depending on irradiation  
 147 channel. All the used standard materials were traceable to SI.

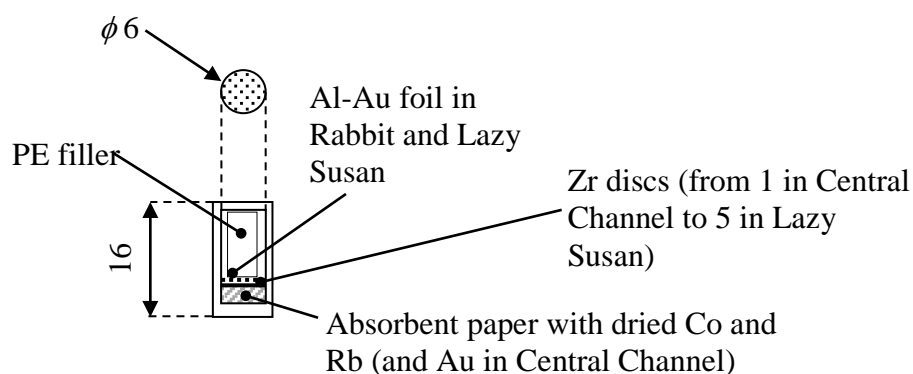
148 Flux monitors were irradiated and left always in the same vial also during the  $\gamma$ -counting  
 149 with the result of a safer and simpler handling of sample in opposition with a longer data  
 150 acquisition. The reason is due to the different activity between short-lived and long-lived  
 151 radionuclides and the convenience to wait for quite complete decay of the firsts for a  
 152 handy acquisition of the seconds. All monitors were put together in a cut 1 mL  
 153 Polyethylene vial of 16 mm height (with cap) and 6 mm internal diameter; Co and Rb  
 154 solutions (and Au in Central Channel irradiation) were pipetted in the vial on a stack of  
 155 12 layers of absorbent paper (width of about 2 mm) and dried with an IR lamp Zr discs



156 were piled above them ranging from 1 disc for Central Channel to 5 discs for Lazy Susan.  
157 Polyethylene filler, a scrap (between 4-5 mm large and 1 mm thick) cut from the wall of a  
158 1 mL vial, was added to avoid misplacing of the setup within the vial in the following  
159 steps. (Fig. 2) shows the sample assembling scheme. Vials were sealed and put (bare or  
160 surrounded by Cd cover) at the bottom of the Polyethylene container used for irradiation.  
161 Io aggiungerei una frase dicendo che probabilmente sia il polietilene dell'irradiation  
162 container, sia del vial con cui hai preparato il campione hanno un effetto termalizzante.  
163 Anche il filler ha effetto termalizzante ma probabilmente con contributo minore date le  
164 dimensione. Al momento questi effetti non sono stati valutati ma, quando nel caso in cui  
165 questo è il setup di normale irraggiamento (e avviene nella maggior parte delle volte) il  
166 valore che stimiamo di  $f$  è quello giusto. Certo che se facessimo l'irraggiamento con il  
167 contenitore di irraggiamento in alluminio oppure senza i vial in PE (penso ad un silicio  
168 tal quale dentro al contenitore) i valori corretti di  $f$  potrebbero essere significativamente  
169 diversi. Sarebbe interessante fare misure di verifica rifacendo tutto usando l'alluminio e  
170 vedendo cosa cambia sul risultato di  $f$ .

171

172 **Fig.2** Monitor set up in an irradiation vial. 1 mL vials cut at the same height were used in  
173 all three irradiation channels. All dimensions are in mm



174

175 For samples diluted enough or for low values of cross sections, as in this case,  $G_{th}$  can be  
176 approximated to 1 with negligible uncertainty. The same holds also for Au in form of foil  
177 due to the high dispersion of gold (0.1%) in the thin Al matrix (0.1 mm) and for Zr in

178 form of disk;  $F_{Cd} = 1$  for great part of nuclides when thickness of Cd cover is 1 mm and  
179 has a cylindrical shape with height to diameter ratio of 2 and sample placed at the center  
180 of the cylinder [5], also in this case uncertainty is considered negligible. Au differs  
181 because of interaction between  $\bar{E}_r$  for Au and Cd main resonance around 0.55 eV. Thus,  
182  $F_{Cd} = 0.991$ .  $G_e$  was calculated according to [5] for Zr ranging from 0.99 in case of 1 disc  
183 to 0.95 in case of 5 piled discs, while, for the other monitors  $G_e = 1$  because of the  
184 dispersion of Co and Rb solutions within the absorbent paper and the high dilution of Au  
185 in solution and solid phase.

186 For the Cd cover, a pure Cd foil with 1 mm thickness was cut and bent in a cylindrical  
187 shape with 18 mm height and 11 mm external diameter; two discs of the same diameter  
188 and 1 mm of thickness were cut and used as upper and lower caps. Cd cylinder was  
189 surrounded with an aluminum foil to maintain correct position among caps and  
190 cylindrical body.

191 The ‘Cd-cover’ irradiation always followed the ‘bare’ one. Delay times between two  
192 subsequent irradiations in the same channel varied from a minimum of 5 min in Rabbit  
193 tube to a maximum of 90 min in Central Channel.

194 All  $\gamma$ -spectra were acquired on a CANBERRA HPGe detector with 35% relative  
195 efficiency and an ORTEC DSPEC 502 multi-channel analyzer. Samples were placed at 6  
196 cm from end-cap of detector to minimize  $\gamma$ -coincidence effects and at the same time to  
197 obtain adequate count rate for every radionuclide; collection time of spectra was adjusted  
198 in order to reach satisfying (i.e.  $\approx 0.5\%$ ) statistical uncertainty due to counting. The net  
199 area of the peaks was obtained from the  $\gamma$ -spectra using the fitting algorithm of the  
200 ORTEC GammaVision 7 software. Energy and efficiency calibration of the detection  
201 system was performed using a point-like multi-gamma source LEA 12ML01EGMA15  
202 placed at the same counting distance.

### 203 (i) Central Channel

204 For what concerns samples preparation, Au solution was used instead of solid standard  
205 because of the extremely low quantities needed in case of use of foil and the subsequent  
206 issues due to possible lack of homogeneity.

207 Both bare and Cd-cover irradiations lasted 30 min. The samples were dropped in the  
208 channel when 20 min have passed after the reactor reached the 250 kW critical power.

209 A long and a short  $\gamma$ -acquisition were acquired for each sample. For the bare, short  
210 counting started 1728 min after irradiation end, lasted 100 min with 7% dead time, while  
211 the long counting started 10005 min after irradiation, lasted 1440 min with dead time  
212 below 1%. The short acquisition of Cd-covered sample started 1745 min after irradiation,  
213 lasted 250 min with 6% dead time while the long acquisition started 1995 min after  
214 irradiation, lasted 2500 min with dead time below 5%.

#### 215 **(ii) Lazy Susan**

216 In this case Au foil was used. It was cut in the shape of a disc with 6 mm diameter. Both  
217 bare and Cd-cover irradiations lasted 30 minutes. Samples were dropped in the channel  
218 when reactor was already at critical power.

219 For the bare, short  $\gamma$ -counting started 1398 min after irradiation end, lasted 67 min with a  
220 6% dead time, while the long counting started 18663 min after irradiation, lasted 3666  
221 min with a dead time below 1%. The short acquisition of Cd-covered sample started 1394  
222 min after irradiation, lasted 67 min with 5% dead time while the longest started 1483 min  
223 after irradiation, lasted 3167 min with dead time below 3%.

#### 224 **(iii) Rabbit**

225 Au foil was cut in the shape of a disc with 6 mm diameter. Three Zr discs were used in  
226 this case.

227 Bare and Cd-cover irradiations lasted 5 minutes. Samples were pneumatically driven in  
228 the channel when reactor was already at critical power as the usual protocol for that kind  
229 of irradiations.

230 The short  $\gamma$ -counting of bare sample started 55 min after the end of irradiation, lasted 73  
231 min with a dead time of 4%; the long acquisition started 130 min after irradiation, lasted  
232 1500 min with similar dead time. Short acquisition for the Cd-covered started 1650 min  
233 after the irradiation, lasted 147 min while the long acquisition started 1798 min after the  
234 irradiation end and lasted 8333 min. In both cases dead time was below 2%.

235 All uncertainties concerning irradiation, decay and counting times were negligible.

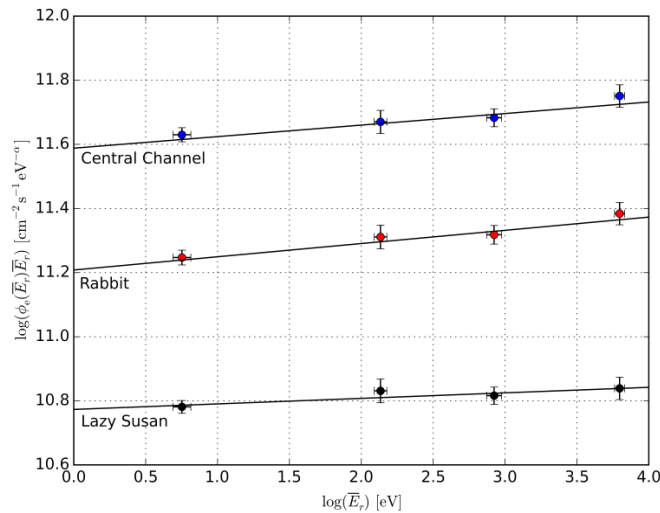
### 236 **Results and discussion**

237 For each set of monitor used in a defined irradiation position, the linear regression  
 238 analysis of the data was performed until convergence to yield numerical values for  $\alpha$ . The  
 239 uncertainty was calculated as described by De Corte [7]. Here and hereafter, uncertainties  
 240 in parentheses ( $k = 1$ ) apply to the last digits.

241 A value of  $\alpha$  equal to  $-0.036(6)$  was found in the Central Channel,  $-0.041(7)$  in the  
 242 Rabbit and  $-0.016(6)$  in the Lazy Susan resulted. In (Fig. 3) the resulting linear  
 243 regression fit on experimental values is showed for all three channels.

244

245 **Fig. 3** Linear regression on data from monitor set in the different irradiation channels are  
 246 showed, uncertainty bars correspond to  $k=2$  confidence level



247

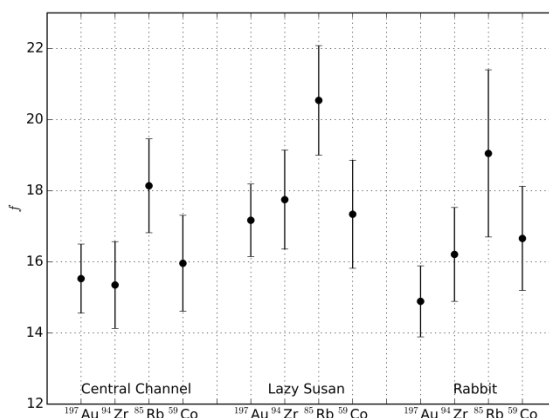
248 The presence of negative values for  $\alpha$  indicates an imperfect thermalization of the  
 249 epithermal part of the neutron flux. Specifically, the epithermal flux in the Central  
 250 Channel and Rabbit tube (i.e. close to reactor core) shows a significant deviation from the  
 251 ideal trend while far from reactor core, as in Lazy Susan channel, it deviates only  
 252 marginally from ideality. This is in agreement with the results obtained in similar  
 253 reactors, as showed in (Table 2).

254 Thermal to epithermal flux ratios were calculated with eq. (7) for the complete monitor  
 255 set in any irradiation channel, and averaged. The  $f$  value deriving from Rb showed a clear

256 offset due to unidentified reasons. Thus, this monitor wasn't included in the average. The  
 257 results of eq. (7) are reported in (Fig. 4) for each monitor element in the three channels.  
 258 Obtained values of  $f$  were 15.6(3) in Central Channel, 17.4(4) in Lazy Susan and 15.7(4)  
 259 in Rabbit pneumatic tube.

260

261 **Fig. 4** Results of using Cd-ratio method from monitor set in different irradiation channels  
 262 are showed, uncertainty bars correspond to  $k=2$  confidence level



263

264 **Table 2** Comparison among evaluation of  $f$  and  $\alpha$  on others TRIGA facilities

	Central Channel		Rabbit		Lazy Susan	
	$f$	$\alpha$	$f$	$\alpha$	$f$	$\alpha$
TRIGA Mark II Pavia (this work)	15.6(3)	-0.036(6)	15.7(4)	-0.041(7)	17.4(4)	-0.016(6)
TRIGA Mark II Ljubljana <sup>[1]</sup>	20.4(8)	-0.051(8)	19.4(7)	-0.048(5)	19.6(8)	-0.009(4)
TRIGA Mark II Morocco <sup>[8]</sup>	-	-	20.0(9)	-0.013(9)	38.3(13)	-0.017(9)

265

266 A trend in the values of  $f$  through the channels of Pavia reactor can be recognized starting  
 267 from the less thermalized Central Channel and arriving to the most thermalized Lazy  
 268 Susan. This particular behavior can be explained with the geometry of the reactor  
 269 concerning the difference between inner irradiation channels (Central Channel and Rabbit  
 270 are inserted in the reactor core) and outer irradiation channel (Lazy Susan is inserted in  
 271 the graphite reflector and is likely to be more affected from the moderation capacity of  
 272 graphite). Discrepancy with Ljubljana reactor  $f$  trend might derive from a different  
 273 arrangement and title of fuel elements (homogeneous 20% enriched <sup>235</sup>U fuel elements in  
 274 the Pavia facility against 20% and 70% enriched <sup>235</sup>U fuel elements interspersed in

275 Ljubljana [1]). However the uncertainties affecting the two series of  $f$  values don't allow  
 276 to have a clearer magnitude of the trends. Moreover, from eq. (8) and eq. (9), values for  
 277  $\Phi_e$  and  $\Phi_{th}$  were obtained and listed in (Table 3). Also the  $f$ ,  $\Phi_e$  and  $\Phi_{th}$  parameters,  
 278 derived from integral flux data reported in [2] and converted according to definition of  
 279 conventional fluxes described in [5], are showed in the same table.

280

281 **Table 3** Thermal and epithermal conventional fluxes values obtained in this work and in  
 282 previous investigations [2] after conversion of relative integral flux data; for the latter set  
 283 of results, also the  $f$  value is showed.

		Central Channel	Rabbit	Lazy Susan
this work	$\Phi_{th} / \text{cm}^{-2} \text{s}^{-1}$	$6.11(16) \times 10^{12}$	$2.54(7) \times 10^{12}$	$1.02(3) \times 10^{12}$
	$\Phi_e / \text{cm}^{-2} \text{s}^{-1}$	$3.92(6) \times 10^{11}$	$1.62(3) \times 10^{11}$	$5.88(9) \times 10^{10}$
[2]	$\Phi_{th} / \text{cm}^{-2} \text{s}^{-1}$	$6.84 \times 10^{12}$	$3.04 \times 10^{12}$	$1.13 \times 10^{12}$
	$\Phi_e / \text{cm}^{-2} \text{s}^{-1}$	$4.26 \times 10^{11}$	$1.90 \times 10^{11}$	$7.93 \times 10^{10}$
	$f$	16.1	16.0	14.2

284

285 Manca commento a: After the results in Table 3, a very short discussion about the  
 286 neutron flux anisotropy in each irradiation channel will be a plus. Declared uncertainties  
 287 for  $f$  and  $\Phi_e$  parameters were evaluated calculating the weighted uncertainty from single  
 288 values obtained with propagation of variances in eq. (7) and eq. (8) respectively. For  
 289 what concerns uncertainty of  $\Phi_{th}$ , it was calculated by propagation of variances of  $f$  and  
 290  $\Phi_e$  in eq. (9). Major contribution to uncertainty of  $f\Phi_e\Phi_{th}$  was found to be due to the  
 291  $Q_0(\alpha)$  values of monitor elements: contribution of  $Q_0(\alpha)$  on uncertainty of each singularly  
 292 calculated  $f$  varied from about 45% for Au to about 85% for Zr and Co in all irradiation  
 293 channels.  $Q_0(\alpha)$  resulted the major uncertainty contribution also in  $\Phi_e$  determination in  
 294 which it was about the 80% of the total for all monitors in every channel; however, in  $f$   
 295 determination, also contribution due to  $(R_{Cd}-1)$  factor is another important component, in  
 296 particular for low thermalized reactors as the TRIGA Mark II is and especially for  
 297 isotopes that prevalently absorb neutrons in the epithermal range (high  $Q_0$ ). In fact, for  $f$   
 298 values calculated from Au, it contributed up to 60% to its uncertainty while for Zr and Co  
 299 (low  $Q_0$ ) the contribution was always below 20%.

300        **Conclusions**

301        With measurement of flux parameters ( $f$  and  $\alpha$ ) at the Pavia TRIGA Mark II reactor, use  
302        of  $k_0$  standardization method can be actually exploited with samples irradiated in this  
303        facility.

304        The comparison of the  $\alpha$  values here reported with those obtained in similar reactors  
305        showed good an agreement. Similarly, the  $f$ ,  $\alpha_{eff}$  and  $\alpha_{th}$  values derived from integral  
306        flux data reported in [2] and converted, were close to the values evaluated in this work. A  
307        relative difference of a few tens of percent was observed in the worst case.

308        **Acknowledgements**

309        This work was funded by the Italian ministry of education, university, and research  
310        (awarded project P6-2013, implementation of the new SI). The authors are much indebted  
311        to Fausto Marchetti and Gabriele Vinciguerra for help during the neutron irradiations and  
312        to Giovanni Magrotti for valuable discussions on historical data concerning the stability  
313        of the reactor power.

314        **References**

- 315        1. Jovanovic S, Smodis B, Jacimovic R, Vukotic P, Stegnar P (1988) Neutron flux  
316        characterisation of the TRIGA Mark II reactor, Ljubljana, Yugoslavia, for use in  
317        NAA. *J Radioanal Nucl Ch.* 129(2): 343-349
- 318        2. Prata M, Alloni D, De Felice P, Palomba M, Pietropaolo A, Pillon M, Quintieri L,  
319        Santagata A, Valente P (2014) Italian neutron sources. *Eur Phys J Plus.* 129(11): 255
- 320        3. Moens L, De Corte F, Simonits A, De Wispelaere A, Hoste J (1979) The effective  
321        resonance energy  $E_r$  as a parameter for the correction of resonance integrals in  $1/E^{1+a}$   
322        epithermal neutron spectra; tabulation of  $E_r$ -values for 96 isotopes. *J Radioanal Nucl*  
323        *Ch.* 52(2): 379-387
- 324        4. Manh Dung H, Yeon Cho S (2003) A simple method for  $\alpha$  determination. *J Radioanal*  
325        *Nucl Ch.* 257(3): 573-575

- 326 5. De Corte F (1987) Habilitation Thesis University of Gent, Belgium
- 327 6. Database of recommended  $k_0$ -data released 11.1.2016 by  $k_0$ -Nuclear Data  
328 Subcommittee of  $k_0$ -International Scientific Committee.  
329 [http://www.kayzero.com/k0naa/k0naaorg/Nuclear\\_Data\\_SC/Entries/2016/1/11\\_New\\_](http://www.kayzero.com/k0naa/k0naaorg/Nuclear_Data_SC/Entries/2016/1/11_New_k0-data_Library_2015.html)  
330 [k0-data\\_Library\\_2015.html](http://www.kayzero.com/k0naa/k0naaorg/Nuclear_Data_SC/Entries/2016/1/11_New_k0-data_Library_2015.html)
- 331 7. De Corte F, Sordo-El Hammami K, Moens L, Simonits A, De Wispelaere A, Hoste J  
332 (1981) The accuracy and precision of the experimental  $\alpha$ -determination in the  $1/E^{1+\alpha}$   
333 epithermal reactor-neutron spectrum. J Radioanal Nucl Ch. 62(1-2): 209-255
- 334 8. Bounouira H, Embarch K, Amsil H, Bounakhla M, Blaauw M (2014) Neutron flux  
335 characterization of the Moroccan Triga Mark II research reactor and validation of the  
336  $k_0$  standardization method of NAA using  $k_0$ -IAEA program. J Radioanal Nucl Ch.  
337 300(2): 465-471